Defect-induced resonance modes in the asymptotic limit of low frequencies: Isotope effects and amplitude patterns*

John B. Page, Jr.
Department of Physics, Arizona State University, Tempe, Arizona 85281
(Received 15 October 1973)

Results are presented of a theoretical study of the harmonic properties of defect-induced low-frequency resonance modes associated with decreased force constants. Some apparently contradictory results of previous authors are resolved. General relations, model-independent and exact in the limit of zero frequency, are established connecting resonance-mode amplitude patterns and frequency shifts accompanying isotopic substitutions for the defect or host atoms. The largest defect isotope shifts turn out to occur when the impurity and host are completely decoupled, in which case the defect behaves as a simple Einstein oscillator. It is shown that the measured shift for the system KBr:Li^+ is incompatible with any harmonic model. The general results are illustrated for a specific model of an isoelectronic substitutional defect in an alkali-halide crystal. The model assumes weakened nearest-neighbor longitudinal force constants at the impurity, and realistic host-crystal phonons are used to numerically compute isotope shifts and amplitude patterns near the defect for a number of systems. The calculated amplitude patterns show clearly that decoupling does not occur for this model. Estimates are made of the computational uncertainties in the calculated defect isotope shifts, and these shifts are compared with the experimental values. For NaCl:Cu^+ and KI:Ag^+, the calculated and observed shifts agree to within experimental error, but it is shown that this error should be reduced before the correctness of the model for these systems can be claimed. The large observed isotope shift for NaI:Cl^- is underestimated by the calculations, and realistic extensions of the model are proposed. The possible role played by anharmonicity for specific systems is briefly discussed.

I. INTRODUCTION

This paper reports the results of a theoretical study of the asymptotic properties of defect-induced harmonic resonances in the zero-frequency limit associated with weakened force constants. Stress is laid upon examining the coupling between impurity and host in this limit and upon the related question of resonance-frequency shifts accompanying isotopic substitutions. The general results are illustrated within the context of a specific defect model, and realistic host-crystal phonons are used to obtain numerical results for some alkali-halide systems.

An impurity-induced resonance is most simply characterized as an in-band analog of a localized mode in the vibrational spectrum of an imperfect crystal. Impurity resonances were first predicted theoretically for pure mass defects,[1] but most of the known systems exhibiting low-frequency resonances involve force-constant decreases. Experimentally, resonances have been studied by means of a number of techniques, among which are measurements of specific heats, thermal conductivity, Raman scattering, and infrared absorption. Experimental and theoretical work done on perturbed phonons up to 1967 is reviewed in articles by Maradudin,[2] Klein,[3] and in the treatise by Maradudin, Montroll, Weiss, and Ipatova.[4] Reference 5 also provides a useful source, for work up to 1968.

Our work is concerned with resonances involving defect motion. For substitutional isoelectronic defects in ionic crystals, such resonances are infrared active, and the first measurements of the infrared absorption due to impurity resonances were reported in 1964 by Sievers[6] and by Weber[7] for substitutional Ag^+ in alkali halides. The infrared properties of low-frequency resonances in a number of alkali halides containing dilute concentrations of substitutional defects have been extensively investigated by Sievers and co-workers[8-13] under a variety of experimental conditions. The second column of Table I lists the frequency ratios they observed for the indicated defect isotope substitutions in NaCl:Cu^+, KI:Ag^+, KBr:Li^+, and NaI:Cl^-. All of the measurements were made at temperatures of 4.2 °K or less. The resonance frequencies for the light impurity isotope in each of the four systems are listed in the first column, and these frequencies are each less than 15% of the maximum host-lattice frequency. The isotopic frequency ratios provide information on the extent to which the defect's surroundings participate in the motion, and in the third column of Table I frequency ratios are listed for the case when the defect behaves as a simple Einstein oscillator. Such behavior would occur in the limiting case of a localized mode of very high frequency since then the impurity would be vibrating alone, but one would not generally

TABLE I. Ratios of resonance frequencies for impurity isotope substitutions. Subscripts l and h denote light and heavy isotopes, respectively. Measured values of the resonance frequencies for the lighter isotopes are listed in the first column, while the experimentally observed frequency ratios are given in column two. Ratios appropriate to Einstein-oscillator behavior are tabulated in the third column. The calculated ratios listed in the fourth column are based upon the defect-nearest-neighbor force-constant change model of Sec. III and were computed using Eq. (30). The quantity F of that equation is a function of just the unperturbed host-crystal phonons, and the values of F listed here were computed from phonons of the breathing shell model.[a] The error estimates given with the calculated frequency ratios are approximate, and their calculation is discussed in Appendix C.

System	ω_l (cm^{-1}) (expt.)	$(\omega_l/\omega_h)_I$ (expt.)	$(m_h/m_l)^{1/2}$	$(\omega_l/\omega_h)_I$ (calc.)	F (amu)
NaCl: $^{63-65}Cu^+$	23.6[b]	1.016[b] ± 0.002	1.0157	1.0142 ± 0.0006	6.97
KI: $^{107-109}Ag^+$	17.4[b]	1.008[b] ± 0.002	1.0093	1.0072 ± 0.0003	30.5
KBr: $^{6-7}Li^+$	17.7[b]	1.105[b] ± 0.004	1.0801	1.015 ± 0.004	26.8
NaI: $^{35-37}Cl^-$	5.4[c]	1.029[c] ± 0.008	1.0282	1.008 ± 0.003	97.6

[a] U. Schröder (Ref. 22).
[b] R. D. Kirby *et al.* (Ref. 8).
[c] B. P. Clayman *et al.* (Ref. 10).

expect such behavior for resonances, as they occur at frequencies within the allowed pass bands of the unperturbed crystal. Nevertheless, one notes from Table I that except for KBr:Li^+, the experimental ratios are very nearly equal to the corresponding Einstein-oscillator ratios, and this suggests that the defect is moving essentially alone in these three systems. The major aim of the present work is to investigate the general relationships between isotope shifts and defect-host coupling in low-frequency resonances.

The harmonic approximation is used throughout this paper. In view of the anomalous properties of the lithium ion in KCl, where it occupies an off-center equilibrium position,[14] it is reasonable to suppose that KBr:Li^+, which is known to be an on-center system, is quite anharmonic. Indeed, we will later prove that the observed isotope shift for KBr: $^{6-7}Li^+$ cannot be explained on the basis of any harmonic model.

For the remaining three systems of Table I, anharmonic effects have been studied experimentally, as will be discussed briefly in Sec. IV, and they have been shown to be important for some properties. As is pointed out in that section, however, the importance of anharmonicity for isotope effects at low temperatures has not been established. The apparent simple Einstein-oscillator ratios observed for these three systems suggest that their low-frequency resonances and associated isotope effects may be understood within the harmonic approximation. Moreover, before anharmonic effects are studied theoretically, it is important that the harmonic behavior be thoroughly understood, and previous studies of low-frequency resonances, made within the harmonic approximation, have led to seemingly contradictory results. These will be discussed in greater detail later on, but suffice it to say here that it has been suggested (i) that Einstein-oscillator behavior might generally hold within the harmonic approximation in the zero-frequency limit,[15,16] (ii) that isotopic frequency ratios greater than those for Einstein-oscillator behavior can occur within a specific harmonic model,[8,17] and (iii) that another specific, but more realistic, model for a perturbed harmonic alkali-halide crystal leads to calculated ratios substantially less than those for Einstein oscillators.[18,3] The primary motivation for the present study was to resolve the apparent conflicts in these results, and all of our work is based upon the harmonic approximation. Furthermore, the work is done for zero temperature and is restricted to dilute concentrations of substitutional defects, so that just the case of a single impurity is considered.

Section II B contains the general theoretical results of the paper. They are derived there without reference to specific assumptions about the nature of the force constant perturbations introduced by the defect and are therefore general within the harmonic approximation. Section II A briefly reviews the usual Lifschitz[19] Green's-function method for perturbed phonons, as it pertains to resonances. This method is used in the model calculations of Sec. III, but the general results of Sec.

II B are derived without recourse to Green's functions.

In Sec. III A, the general results are illustrated within the context of a specific defect model, while in Sec. III B the results of numerical calculations based upon this model and realistic host crystal phonons are presented and discussed for several alkali-halide systems. Results for isotope shifts and for amplitude patterns are presented, as are theoretical uncertainty estimates for the shifts. Such estimates turn out to be necessary before a meaningful comparison of theoretical and experimental isotope shifts can be made.

Klein[3] and Benedek and Nardelli[18] have used a similar defect model, but different host crystal phonons, to study low-frequency resonances in some systems, and our numerical studies extend their work. These authors were the first to point out that a very light impurity associated with sufficiently weakened force constants could give rise to both a high-frequency localized mode and a low-frequency resonance, provided that long-range force constants are present in the system. They did not calculate the amplitude patterns associated with resonances, nor did they give theoretical uncertainty estimates, but their calculations showed the possibility of substantial coupling between the defect and host at low frequencies for this model. The extent to which this is so in a number of systems is revealed by our calculated amplitude patterns.

The discussion of our numerical results begun in Sec. III B is continued in Sec. IV. Suggested directions that future work might take are also discussed in that section, and Sec. V consists of a brief summary of the paper.

II. GENERAL THEORY

A. Formal background

The notation is similar to that used previously by the author.[20] The basic eigenvalue problem of the harmonic approximation is

$$(\underline{\Phi} - \omega_f^2 \underline{M})\underline{\chi}(f) = 0 , \tag{1}$$

where $\underline{M}$ and $\underline{\Phi}$ are the system's mass and harmonic force constant matrices and f labels the normal modes. The eigenvectors $\underline{\chi}(f)$ give the particle amplitudes for each normal mode and are orthonormal with respect to $\underline{M}$,

$$\tilde{\underline{\chi}}(f)\underline{M}\,\underline{\chi}(f') = \delta_{ff'} . \tag{2}$$

Although Green's functions will not be used until Sec. III, the notion of a resonance is most easily introduced in terms of the system's harmonic Green's-function matrix

$$\underline{G}(\omega^2) = (\underline{\Phi} - \omega^2 \underline{M})^{-1} = \sum_f \underline{\chi}(f)\tilde{\underline{\chi}}(f)(\omega_f^2 - \omega^2)^{-1} . \tag{3}$$

The equivalence of these two forms follows at once from the use of Eq. (1) and the completeness relation $\sum_f \underline{M}\,\underline{\chi}(f)\tilde{\underline{\chi}}(f) = \underline{I}$. The Green's function is related to the system's linear response to an applied electric field, provided that the dipole moment operator of the system is linear in the particle displacements $\underline{u} = \{u(n\alpha)\}$. In this case it is a straightforward exercise in linear response theory to show that the imaginary part of the dielectric susceptibility at frequency ω is proportional to the Fourier transform $\langle \underline{u}\tilde{\underline{u}} \rangle^{\omega}$ of the displacement-displacement correlation matrix $\langle \underline{u}(t)\tilde{\underline{u}} \rangle$, where the brackets denote a thermal average and $\underline{u}(t)$ is the displacement operator expressed in the Heisenberg representation at time t. In the harmonic approximation, one obtains

$$\langle \underline{u}\tilde{\underline{u}} \rangle^{\omega} = \pi^{-1}\hbar n(\omega)\,\mathrm{Im}\underline{G}(z) , \tag{4}$$

where $n(\omega) = (e^{\beta\hbar\omega} - 1)^{-1}$ is the Planck distribution function and ω is assumed positive. The variable z is equal to $\omega^2 + i\epsilon$, and the limit $\epsilon \to 0^+$ is understood.

If a substitutional impurity is present in the lattice, the mass and force constant matrices may be written $\underline{M} = \underline{M}_0 + \Delta\underline{M}$ and $\underline{\Phi} = \underline{\Phi}_0 + \Delta\underline{\Phi}$, with $\underline{M}_0$ and $\underline{\Phi}_0$ referring to the unperturbed crystal. It then follows from the first part of Eq. (3) that the Green's-function matrices for the perturbed and unperturbed crystal are related through

$$\underline{G}(z) = [\underline{I} + \underline{G}_0(z)\underline{C}(z)]^{-1}\underline{G}_0(z) , \tag{5}$$

where the perturbing matrix $\underline{C}(z)$ is equal to $\Delta\underline{\Phi} - z\Delta\underline{M}$. Elements of the real and imaginary parts of the unperturbed Green's-function matrix $\underline{G}_0(z)$ may be numerically computed from the host crystal phonon frequencies and polarization vectors. This will be discussed further when numerical calculations are taken up in Sec. III B.

Comparison of Eqs. (4) and (5) shows that $\langle \underline{u}\tilde{\underline{u}} \rangle^{\omega}$ is proportional to the quantity $[(\mathrm{Re}|\underline{I} + \underline{G}_0(z)\underline{C}(z)|)^2 + (\mathrm{Im}|\underline{I} + \underline{G}_0(z)\underline{C}(z)|)^2]^{-1}$, with the bars indicating determinants. The condition for a resonance is the vanishing of this quantity's first term, and this condition is equivalent to

$$\mathrm{Re}|\underline{1} + \underline{g}_0(z)\underline{c}(z)| = 0 . \tag{6}$$

Here $\underline{1}$, $\underline{g}_0(z)$, and $\underline{c}(z)$ are the submatrices of $\underline{I}$, $\underline{G}_0(z)$, and $\underline{C}(z)$ in the "impurity" subspace, defined by the sites associated with nonzero elements of $\underline{C}(z)$. In problems of practical interest, such as that of an isoelectronic defect in an alkali halide crystal, the force constant changes may be limited to a relatively small number of particles near the defect so that the determinant in Eq. (6) involves

a matrix of manageable dimensions.

Note that only the real part of $\underline{c}(z)$ survives in the limit $\epsilon \to 0^+$, and that for ω outside the unperturbed frequency bands the imaginary part of $\underline{g}_0(z)$ vanishes. Thus, for such frequencies the resonance condition (6) becomes simply $|\underline{1} + \underline{g}_0(\omega^2)\underline{c}(\omega^2)| = 0$, which is the usual condition for the appearance of a localized mode. For ω within the unperturbed frequency bands, the resonance condition can result in maxima in the elements of $\langle \underline{u}\underline{\tilde{u}} \rangle^\omega$ and hence a maximum in the linear response of the system to an applied electric field. Moreover, since the diagonal elements of $\langle \underline{u}\underline{\tilde{u}} \rangle^\omega$ give the contribution per unit frequency from modes in $(\omega, \omega + d\omega)$ to the mean-square particle displacements $\langle u^2(n\alpha) \rangle$, the resonance condition can result in maxima in these quantities. However, whether or not maxima actually occur in either the mean-square displacements or the susceptibility depends upon the behavior of the entire imaginary part of the perturbed Green's function $\underline{G}$ near the resonance frequency.

This paper is concerned with the behavior of resonances involving impurity motion. For definiteness, a substitutional impurity in a crystal of the rocksalt structure will be studied. The point group is O_h, and only the threefold degenerate $T_{1u}(\Gamma_{15})$ modes involve impurity motion. We will consider x-polarized T_{1u} modes, and for these $u(0x)$ is nonzero, where $n = 0$ labels the defect site. In practice the matrices in Eq. (6) are to be expressed in an x-polarized T_{1u} symmetry basis, but because an explicit model calculation will not be performed until Sec. III, the introduction of a symmetry basis will be deferred to that section.

The notion of a resonance at zero frequency will play a central role in our work. For a finite defect mass and in the $\omega \to 0$ limit, $\underline{c}(z)$ approaches $\Delta\underline{\phi}$, and the resonance condition becomes simply

$$|\underline{1} + \underline{g}_0(0)\Delta\underline{\phi}_c| = 0 . \tag{7}$$

Here $\Delta\underline{\phi}_c$ signifies any force-constant perturbation matrix satisfying this equation, and $\underline{g}_0(0)$ is the $\omega = 0$ limit of just the real part of $\underline{g}_0(z)$ since the imaginary part vanishes in this limit, as may be seen from the arguments of Appendix A. For a given model of the force constant perturbations, Eq. (7) is the condition on the elements of $\Delta\underline{\phi}$ for the appearance of a resonance at zero frequency. This condition is independent of the system's masses, and in Sec. III B we will see that for the model of changed longitudinal overlap force constants between the impurity and its nearest neighbors, Eq. (7) holds for weakenings of typically 60% in a number of alkali halides. Larger decreases would result in an instability for T_{1u} modes—the system would distort to a new equilibrium configuration. The off-center KCl:Li^+ system[14] presumably could be an example of such behavior.

The zero-frequency resonance condition (7) is equivalent to $|\underline{I} + \underline{G}_0(0)\Delta\underline{\Phi}_c| = 0$, and because $\underline{G}_0(0)$ is just $\underline{\Phi}_0^{-1}$, this is the necessary and sufficient condition for the existence of non-trivial solutions of the equation

$$(\underline{\Phi}_0 + \Delta\underline{\Phi}_c)\underline{\chi}(f) = 0 , \tag{8}$$

which is the $\omega_f \to 0$ limit of the basic eigenvalue equation (1). Of course, if the system is invariant to arbitrary uniform translations, Eq. (8) will always have nontrivial solutions corresponding to uniform translations, regardless of the value of $\Delta\underline{\Phi}_c$. However, we will be confining our attention to the behavior of low frequency resonances in the $\omega \to 0$ limit associated with the approach of the force constant perturbation matrix $\Delta\underline{\Phi}$ to a critical value $\Delta\underline{\Phi}_c$, and for these bona fide vibrations the system's center of mass is at rest, the eigenvectors $\underline{\chi}(f)$ are orthogonal (with respect to $\underline{M}$) to uniform translations, and $\underline{\Phi}_0\underline{\chi}(f)$ is nonzero.

It should be noted that a resonance at zero frequency can also be obtained by letting the defect mass go to infinity, as is intuitively clear. Such "mass-induced" low-frequency resonances have been thoroughly discussed in the literature,[16] and we will continue to focus on the more interesting and complex case of low-frequency resonances associated with large force-constant weakenings.

B. Isotope shifts

Having set down the formal basis for the remainder of the paper, let us now suppose that the system's mass matrix $\underline{M}$ is altered to $\underline{M}'$ via substitutional mass perturbations, involving any or all of the system's sites. Although the changes in $\underline{M}$ are not assumed to be localized, it is assumed that these perturbations are not accompanied by any changes in $\underline{\Phi} = \underline{\Phi}_0 + \Delta\underline{\Phi}$, the system's force-constant matrix.

Since just modes having nonzero defect amplitudes are being considered, one can introduce vectors $\underline{\mathfrak{A}}(f)$ giving the normalized particle amplitudes relative to that of the defect

$$\underline{\chi}(f) = \underline{\mathfrak{A}}(f)\chi(0x|f) . \tag{9}$$

When expressed in terms of $\underline{\mathfrak{A}}(f)$, the basic eigenvalue equation (1) is

$$\underline{\Phi}\underline{\mathfrak{A}}(f) = \lambda_f \underline{M}\underline{\mathfrak{A}}(f) , \tag{10}$$

where λ_f stands for ω_f^2. This equation can be used to express λ_f as $\lambda_f = \tilde{\underline{\mathfrak{A}}}(f)\underline{\Phi}\underline{\mathfrak{A}}(f)/\tilde{\underline{\mathfrak{A}}}(f)\underline{M}\underline{\mathfrak{A}}(f)$, which is of the usual harmonic oscillator form $\lambda_f = k_f^*/m_f^*$, but with the effective mass and force

constant being determined from $\underline{M}$ and $\underline{\Phi}$ by the relative amplitude vector $\underline{\mathfrak{A}}(f)$.

Instead of restricting ourselves to low frequencies at the outset, let us for the time being consider the effect of an arbitrary change in the product $\lambda_f \underline{M} \equiv \underline{x}_f$ for a mode f of any frequency. With the basic eigenvalue equation (10) being written before and after the change as $\underline{\Phi}\underline{\mathfrak{A}}(f) = \underline{x}_f \underline{\mathfrak{A}}(f)$ and $\underline{\Phi}\underline{\mathfrak{A}}'(f) = \underline{x}'_f \underline{\mathfrak{A}}'(f)$, respectively, a straightforward calculation leads to the identity

$$\tilde{\underline{\mathfrak{A}}}(f)(\underline{x}_f - \underline{x}'_f)\underline{\mathfrak{A}}'(f) = 0 . \tag{11}$$

For the case when the changes $\underline{M}' - \underline{M}$, $\underline{\mathfrak{A}}'(f) - \underline{\mathfrak{A}}(f)$, and $\lambda'_f - \lambda_f$ are small compared with the corresponding initial values, one obtains the first-order result

$$\lambda_f / \lambda'_f = \tilde{\underline{\mathfrak{A}}}(f)\underline{M}'\underline{\mathfrak{A}}(f) / \tilde{\underline{\mathfrak{A}}}(f)\underline{M}\underline{\mathfrak{A}}(f) . \tag{12}$$

If the mass changes are sufficiently small, this perturbation theory result gives a good approximation to λ_f / λ'_f for a mode f of arbitrary frequency. However, note that if the difference $\underline{\mathfrak{A}}'(f) - \underline{\mathfrak{A}}(f)$ were to vanish, Eq. (11) would lead identically to Eq. (12) with no approximations involved. It turns out that this happens in the low-frequency limit—as one looks at progressively lower frequencies associated with force constant weakening, Eq. (12) gives a better and better approximation to λ_f / λ'_f and becomes exact in the zero-frequency limit, *regardless of* $\underline{M}'$. In order to further clarify the low-frequency case and to keep the general work of this section parallel with the model calculations of Sec. III A, a separate derivation of the low-frequency version of Eq. (12) will now be given.

The effect of the change $\underline{M} \to \underline{M}'$ on a very low-frequency resonance will be studied by investigating the behavior of the normal mode f for which λ_f approaches zero as $\Delta\underline{\Phi}$ approaches $\Delta\underline{\Phi}_c$, the value satisfying the determinental condition $|\underline{\Phi}_0 + \Delta\underline{\Phi}_c| = 0$, implied by Eq. (8). We write $\underline{\Phi} = \underline{\Phi}_0 + \Delta\underline{\Phi}_c + (\Delta\underline{\Phi} - \Delta\underline{\Phi}_c)$ and $\underline{\mathfrak{A}}(f) = \underline{A}(f) + [\underline{\mathfrak{A}}(f) - \underline{A}(f)]$, where $\underline{A}(f)$ is the zero-frequency limit of $\underline{\mathfrak{A}}(f)$. The vector $\underline{A}(f)$ will play an important role in our work and is determined by the equation

$$(\underline{\Phi}_0 + \Delta\underline{\Phi}_c)\underline{A}(f) = 0 , \tag{13}$$

together with the condition $A(0x|f) = 1$. Thus, the relative amplitudes at zero frequency are *independent* of the system's masses. The identity $\tilde{\underline{A}}(f)(\Delta\underline{\Phi} - \Delta\underline{\Phi}_c)\underline{\mathfrak{A}}(f) = \lambda_f \tilde{\underline{A}}(f)\underline{M}\underline{\mathfrak{A}}(f)$ follows from Eq. (10), and for a sufficiently low frequency $\underline{\mathfrak{A}}(f) - \underline{A}(f)$ will be small compared with $\underline{A}(f)$. The first-order result for small λ_f is

$$\lambda = \tilde{\underline{A}}(\Delta\underline{\Phi} - \Delta\underline{\Phi}_c)\underline{A} / \tilde{\underline{A}}\underline{M}\underline{A} , \tag{14}$$

where the mode index f has been dropped. Throughout the remainder of this paper we will continue to neglect terms nonlinear in λ in the frequency condition for low-frequency modes. This means that the isotope frequency ratios or fractional shifts to be derived will contain just zeroth order terms in λ and hence will be exact at $\lambda = 0$. Numerical evidence will be given in Sec. III B that working in the linear frequency regime is adequate for the experimental resonances of Table I.

Under an isotopic substitution $\underline{M} \to \underline{M}'$, the only quantity on the right-hand side of Eq. (14) that changes is $\underline{M}$ itself, and one has

$$L(\lambda/\lambda') = \tilde{\underline{A}}\underline{M}'\underline{A} / \tilde{\underline{A}}\underline{M}\underline{A} , \tag{15}$$

where the symbol L signifies that this is an exact result for arbitrary $\underline{M}'$ in the limit $\lambda \to 0$ [or whenever the linear approximation (14) is exact]. Equation (15) is the low-frequency version of the previously derived perturbation-theory result (12). The general orthonormality condition (2) leads to the relation

$$\chi^{-2}(0x|\lambda = 0) = \tilde{\underline{A}}\underline{M}\underline{A} \tag{16}$$

at $\lambda = 0$, and this equation together with the fact that the zero-frequency relative amplitude vector $\underline{A}$ is mass independent, allows Eq. (15) to be rewritten

$$L(\lambda/\lambda') = [\chi(0x|\lambda = 0)/\chi'(0x|\lambda = 0)]^2 .$$

Equation (15) and, indeed, all of the expressions of this subsection are general within the harmonic approximation, holding equally well for perfect lattices, lattices with impurities, or disordered lattices, as long as $\underline{\mathfrak{A}}(f)$ gives the displacements relative to that on a particle whose amplitude is nonzero. However, in this paper we will stay within the context of a single substitutional impurity.

1. *Impurity-isotope shift*

Consider now the case of an isotopic substitution for the impurity such as, for example, the replacement of $^{63}Cu^+$ by $^{65}Cu^+$ in the NaCl:Cu^+ system. Equation (15) yields

$$L(\lambda/\lambda')_I = (m'_I + S)/(m_I + S) , \tag{17}$$

where m_I stands for the impurity mass and the S is the sum

$$S = \sum_{\alpha, n \neq 0} m_n A^2(n\alpha) . \tag{18}$$

A subscript I has been added to $L(\lambda/\lambda')$ to distinguish this isotope shift from the "host" shift to follow. Since the sum S involves only positive quantities, one immediately obtains for the case of a heavy isotope the inequality

$$L(\lambda/\lambda')_I \leq m_I'/m_I, \tag{19}$$

with the equality holding only for all $A(n\alpha)=0$ for $n\neq 0$. In other words, in the harmonic approximation, but regardless of the details or extent of the harmonic-force-constant perturbations, Einstein-oscillator behavior is an upper limit on $L(\lambda/\lambda')_I$ and holds if and only if just the defect is moving as λ approaches zero.

Although Eqs. (17)–(19) have been derived in the low-frequency limit, where they are exact for *any* m_I', it is apparent from a comparison of Eqs. (12) and (15) that with $\underline{\mathcal{A}}(f)$ replacing $\underline{A}$, these three equations also hold to first order in $(m_I'-m_I)$ for a mode f of arbitrary frequency.

From the preceding inequality (19), we can immediately conclude that the measured KBr:$^{6-7}$Li$^+$ isotope shift cannot be understood within the harmonic approximation, since a comparison of the data of columns 2 and 3 of Table I shows the observed frequency ratio for this system to be much greater than that for Einstein-oscillator behavior. Thus KBr:Li$^+$ must be regarded as a very anharmonic system.

Sievers and Takeno[17] have derived a model-dependent expression for the squared frequency λ of a low-frequency impurity resonance, and their result leads to a ratio $(\lambda/\lambda')_I$, which is greater than the Einstein-oscillator limiting value m_I'/m_I predicted by our general result (19). However, as is shown in Appendix B, their expression for λ contains some, but not all, terms of second and higher order in λ, and when these are eliminated their model predicts $L(\lambda/\lambda')_I = m_I'/m_I$, which is consistent with our general result. It is furthermore shown in Appendix B that when their model is used to calculate λ consistently even to *second* order, the ratio $(\lambda/\lambda')_I$ so obtained again turns out to be given by the Einstein-oscillator value m_I'/m_I. In the Sievers-Takeno model the host lattice is assumed to involve just equal nearest-neighbor longitudinal and transverse force constants $k_l = k_t \equiv k$, and the impurity is assumed to perturb only the force constants $k_{lI} = k_{tI} \equiv k_I$ to its six-nearest neighbors. Since the force constants in this model are all positive and couple just nearest neighbors, it is clear that a zero-frequency resonance may be achieved only by reducing k_I to zero and that the defect and host are decoupled in this situation, so that Einstein-oscillator behavior necessarily results. On the other hand, we will see in Sec. III B that calculations of $L(\lambda/\lambda')_I$ for alkali halides and based upon shell model phonons lead to values significantly less than those appropriate to an Einstein oscillator. This is because with realistic force constant models for alkali halides, the defect and host remain coupled in the zero-frequency limit, so that the relative amplitudes $A(n\alpha)$ are nonzero on the host ions. Hence in view of Eqs. (17) and (18), S is nonzero and $L(\lambda/\lambda')_I$ involves more than just the impurity mass.

Krumhansl[15] and Krumhansl and Matthew[16] have argued that Einstein-oscillator behavior may be a rather general property of impurity resonances in the low-frequency limit. This conclusion was based upon the neglect of force constant elements $\Phi(0\alpha, n\beta)$ coupling the impurity to other particles $(n\neq 0)$ in the lattice, but these authors cautioned that this assumption might not be justified for ionic crystals. Our numerical results imply that these force constant elements are often large in alkali halides, as mentioned in the previous paragraph. Indeed, the results of this paper show that Einstein-oscillator behavior is by no means a necessary general asymptotic property of low-frequency harmonic resonances.

2. *Host-isotope shift*

We will now leave the problem of isotopic substitutions for the impurity and will instead consider the effect on a low-frequency impurity-induced resonance of making an isotopic substitution in the entire host lattice. An example of this would be the substitution $^{35}Cl^- \rightarrow {}^{37}Cl^-$ in the NaCl:Cu$^+$ system. We will make the simplifying assumption that the fractional mass perturbation is the same for each particle in the host crystal. Thus it is assumed that the change $\Delta m_l = m_l' - m_l$ of the host-ion mass at site l is given by γm_l, where γ is independent of l. This is, of course, exactly true for a monatomic host.

Applying the basic result (15) to this situation, one has

$$L(\lambda/\lambda')_H = \underline{\tilde{A}}\,\underline{M}'\,\underline{A}/\underline{\tilde{A}}\,\underline{M}\,\underline{A} = [m_I + (1+\gamma)S]/(m_I + S), \tag{20}$$

where S is the sum defined in Eq. (18). Since this sum also occurs in our expression (17) for the defect-isotope effect, we can easily relate the two types of shifts. The result can be expressed as

$$L\left(\frac{\Delta\lambda}{\lambda}\right)_H = -\frac{\gamma[L(\lambda/\lambda')_I - m_I'/m_I]}{1 - m_I'/m_I + \gamma[L(\lambda/\lambda')_I - m_I'/m_I]}, \tag{21}$$

where m_I and m_I' are the masses involved in the impurity-isotope substitution. Again, this is a general harmonic result and is hence independent of the nature of the force constants in the system. Moreover, this equation relates the two types of isotope shifts through just the masses involved. Were measured host shifts available and sufficiently accurate, such a relation could offer a useful

consistency check on the use of the harmonic approximation.

Again by comparing Eqs. (12) and (15), it is seen that Eq. (20), which holds for arbitrary γ in the low-frequency limit, also gives the ratio $(\lambda/\lambda')_H$ to first order in γ for a mode f of arbitrary frequency if the replacement $\underline{A} \to \underline{\mathfrak{A}}(f)$ is made in the sum S.

According to Eq. (21) the host isotope shift $L(\Delta\lambda/\lambda)_H$ vanishes when the impurity-isotope shift exhibits Einstein-oscillator behavior; that is, when $L(\lambda/\lambda')_I$ is equal to m_I'/m_I. This result is consistent with our earlier result that Einstein-oscillator behavior for $L(\lambda/\lambda')_I$ means that just the impurity is moving and, in fact, holds *regardless* of how the host mass change is distributed over the lattice. This follows from Eq. (15) together with the relation $A(nx) = \delta_{n0}$ implied by Einstein-oscillator behavior of $L(\lambda/\lambda')_I$. For any host-isotopic substitution one then has $L(\lambda/\lambda')_H = 1$ and hence $L(\Delta\lambda/\lambda)_H$ is zero.

3. *Impurity amplitude*

If the normalization condition (16) is combined with the result (17) for the impurity-isotope effect, the squared normalized impurity amplitude at zero frequency can be expressed as

$$\chi^2(0x\,|\,\lambda = 0) = [\,L(\lambda/\lambda')_I - 1]/(m_I' - m_I)\,. \qquad (22)$$

When $L(\lambda/\lambda')_I$ is equal to m_I'/m_I, one has $\chi^2(0x\,|\,\lambda = 0) = m_I^{-1}$, which by the normalization condition again means that the defect is moving alone.

III. THEORY AND NUMERICAL RESULTS FOR A SIMPLE DEFECT MODEL

The general results of Sec. II B are based solely upon the fundamental lattice dynamics equations (1) and (2) and involve no Green's functions. However, when studying specific force-constant models, the Green's function formalism reviewed in Sec. II A provides a tractable theoretical approach in that only impurity subspace vectors and matrices need to be considered. Accordingly we will now return to the Green's-function formalism and investigate low-frequency resonances within the context of an explicit model for the force-constant perturbations introduced by the defect. In this way the preceding general results will be set in the framework of a specific model, and numerical calculations can be carried out.

For an isoelectronic substitutional impurity in an ionic crystal of the NaCl structure, the simplest first approximation is to consider just longitudinal force-constant changes $\delta = k_I' - k_I$ between the defect and each of its six nearest neighbors. These changes may be thought of as arising from altered overlap interactions, but also note that because of anharmonicity, short-range as well as Coulomb force constants will be perturbed by any lattice distortion accompanying the defect. Such changes are implicitly included in δ, but for simplicity we will ignore relaxation-induced force constant changes beyond nearest neighbors. These perturbations can be rather extensive,[21] and their effects will be discussed elsewhere.

A. Theory

The sites occurring in the impurity subspace are those of the impurity and its six nearest neighbors. For the assumed longitudinal force-constant perturbations, there are but two linearly independent x-polarized T_{1u} symmetry basis vectors in the impurity subspace, and we will use the normalized basis shown in Fig. 1, which also gives the labeling convention. Expressed in this basis, the impurity-subspace unperturbed Green's-function matrix is given by

$$\underline{g}_0{}^B(z) = \{\underline{\tilde{\xi}}(T_{1u}t)\underline{g}_0(z)\underline{\xi}(T_{1u}t')\} = \begin{pmatrix} G_0(1x,1x;z) + G_0(1x,-1x;z) & \sqrt{2}\,G_0(0x,1x;z) \\ \sqrt{2}\,G_0(0x,1x;z) & G_0(0x,0x;z) \end{pmatrix}, \qquad (23)$$

where point symmetry arguments have been used to minimize the number of independent elements. Since we are only concerned with matrices and vectors expressed in the illustrated symmetry basis, the superscript B can be dropped. For the assumed force constant changes, the impurity-subspace perturbing matrix in our basis is

$$\underline{c}(z) = \begin{pmatrix} \delta & -\sqrt{2}\,\delta \\ -\sqrt{2}\,\delta & 2\delta - z\Delta m \end{pmatrix}. \qquad (24)$$

The quantity $\Delta m \equiv m_I - m_0$ represents the mass change associated with the introduction of the impurity into the lattice. With $\underline{g}_0(z)$ and $\underline{c}(z)$ given by the preceding two equations, Eq. (6) yields the resonance condition

$$\mathrm{Re}\{\,\delta(2G_2(z) - G_1(z)) + 1 + z\Delta m[\,\delta(G_0(0x,0x;z)G_1(z) - 2G_0(0x,1x;z)G_2(z)) - G_0(0x,0x;z)]\,\} = 0, \qquad (25)$$

where $G_1(z)$ and $G_2(z)$ stand for $2G_0(0x,1x;z) - G_0(1x,1x;z) - G_0(1x-1x;z)$ and $G_0(0x,0x;z) - G_0(0x,1x;z)$,

respectively. The variable z is of course $\omega^2 + i\epsilon$, with the limit $\epsilon \to 0^+$ understood.

We are interested in the solution of the above equation for $\omega \to 0$. As is seen in Appendix A, the imaginary parts of the Green's-function elements vanish in this limit, whereas the real parts in general do not. Thus, to first order in $\lambda = \omega^2$, the Green's functions in the square brackets of Eq. (25) may be replaced by their real parts at zero frequency. Moreover, it is shown in Appendix A that within a simple Debye approximation the real parts of $G_1(z)$ and $G_2(z)$ are linear in λ in the low-frequency limit. Expanding the real part of $2G_2(z) - G_1(z)$ about $\lambda = 0$ and dropping from the resonance condition (25) terms in which nonlinear powers of λ appear explicitly, one obtains the low-frequency approximation

$$\lambda = \frac{1 + \delta(2G_2 - G_1)}{\Delta m\{\delta[2G_2G_0(0x, 1x) - G_1G_0(0x, 0x)] + G_0(0x, 0x)\} - \delta[D_\lambda(2G_2 - G_1)]} \tag{26}$$

for the squared resonance frequency. Here the real parts of the Green's-function elements and their derivatives with respect to λ are evaluated at $\lambda = 0$, and this is signified by the omission of the argument z from these quantities. According to Eq. (26), the resonance frequency approaches zero for two limiting situations, one of which is the limit $\Delta m \to \infty$ of a very heavy defect. In this case λ approaches zero for any value of δ. Furthermore, it is easy to see from Eq. (26) that such "mass-induced" low-frequency resonances lead to Einstein-oscillator impurity-isotope frequency shifts, as one would expect.

The second and more interesting situation leading to a zero-frequency resonance occurs when the force-constant perturbation approaches the critical value

$$\delta_c = -(2G_2 - G_1)^{-1}, \tag{27}$$

and this is the case with which we are concerned in this paper. Any further change of δ results in an imaginary resonance frequency, meaning that with the impurity equilibrium position at the substitutional lattice site as assumed, the system is unstable. The critical value of δ is independent of the system's masses and is determined solely by the host-crystal force constants through the real parts of the unperturbed Green's-function elements $2G_2 - G_1$. For any general defect model involving a finite impurity mass, the application of the zero-frequency resonance condition will obviously reduce by one the number of independent parameters characterizing the force constant perturbations, and hence in the present model the zero-frequency condition completely determines $\Delta\Phi_c$.

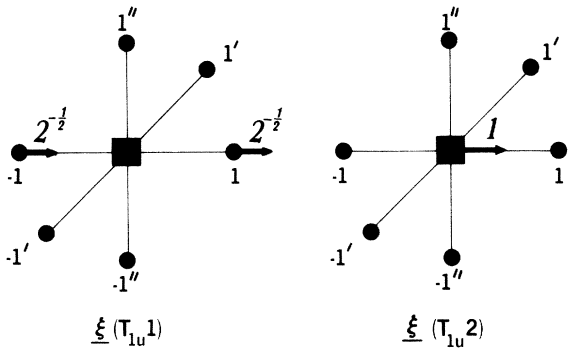

FIG. 1. Normalized impurity-subspace basis vectors of T_{1u} symmetry, polarized in the x direction.

The low-frequency approximation (26) contains terms nonlinear in λ. When the force constant perturbation δ is close to the critical value δ_c, we write $\delta = \delta_c + (\delta - \delta_c)$ and retain in Eq. (26) just terms of first order in $\delta - \delta_c$. This yields the condition

$$\lambda = \tfrac{1}{2}(\delta - \delta_c)[(G_1/G_2) - 2]^2/(m_I + F), \tag{28}$$

where use has been made of Eq. (27), and the quantity F is defined by

$$F = D_\lambda(2G_2 - G_1)/2G_2^2 - m_0. \tag{29}$$

Equation (28) is the first-order result for a "force-constant-induced" low-frequency resonance and is just the general harmonic first-order expression (14) of Sec. II B written in terms of the present model, as will be demonstrated in the particle amplitude portion of the present section.

1. *Impurity-isotope shift for the model*

If the squared-resonance frequency λ is described by the linear approximation (28) both before and after an isotopic substitution $m_I \to m_I'$ of the impurity, the ratio $(\lambda/\lambda')_I$ is given by

$$L(\lambda/\lambda')_I = (m_I' + F)/(m_I + F). \tag{30}$$

Comparison of this result with the general harmonic expression (17) of Sec. II B shows that the quantity F must be equal to the sum S defined by Eq. (18). That this equality explicitly follows from the present model will be shown when the subject of particle amplitudes is taken up.

According to Eq. (30), the necessary and sufficient condition for an Einstein-oscillator defect-

isotope shift in this model is the vanishing of the quantity F. Note that this is a condition involving just host lattice quantities. As has been mentioned, the neglect of nonlinear terms in the low-frequency resonance condition results in isotope-frequency ratios or fractional shifts that are valid to zeroth order in λ and are therefore exact at $\lambda = 0$. Since the force-constant perturbations of the present model are completely fixed by the $\lambda = 0$ condition, expression (30) for $L(\lambda/\lambda')_I$ contains no free model parameters, and the occurrence or nonoccurrence of Einstein-oscillator behavior is solely a property of the host. For a more general defect model, the zeroth order expression for the isotope-frequency ratio would involve all but one of the independent force-constant perturbation parameters, with the remaining parameter being determined by the $\lambda = 0$ condition.

2. *Host-isotope shift for the model*

As in Sec. II B, it will be assumed that the host-lattice isotopic substitution is of the form $\underline{M}_0 \rightarrow \underline{M}_0' = (1+\gamma)\underline{M}_0$, where γ is a scalar. Such a change has a simple effect upon the Green's-function matrix: $\underline{G}_0'(z) = [\underline{\Phi}_0 - z(1+\gamma)\underline{M}_0]^{-1} = \underline{G}_0[z(1+\gamma)]$. Again using the results of Appendix A that the real parts of $G_1(z)$ and $G_2(z)$ and their derivatives with respect to λ are well behaved at $\lambda = 0$, one has

$$G_i'(\lambda) = G_i + \lambda(1+\gamma)D_\lambda G_i + \dot{O}(\lambda^2) , \tag{31}$$

where G_i stands for either G_1 or G_2. This result is valid for any fractional host mass perturbation γ.

One can now work out the low-frequency resonance condition analogous to Eq. (28), but for a defect of mass m_I and force-constant change δ in the isotopically perturbed *host* crystal. Equation (31) shows that the perturbed zero-frequency host-lattice quantities G_1', G_2', and F are given by G_1, G_2, and $(1+\gamma)F$, respectively, so that Eq. (28) leads to

$$\lambda' = \tfrac{1}{2}(\delta - \delta_c)(G_1/G_2 - 2)^2/[m_I + (1+\gamma)F] . \tag{32}$$

Combining this result with Eq. (28) gives

$$L(\lambda/\lambda')_H = [m_I + (1+\gamma)F]/(m_I + F) . \tag{33}$$

When F is eliminated between this equation and Eq. (30) for $L(\lambda/\lambda')_I$, the result is equivalent to Eq. (21), and hence that general harmonic result has been explicitly verified for this model.

3. *Amplitudes for the model*

We have previously noted that the vector $\underline{A}$, which gives the zero-frequency amplitudes relative to that of the impurity, is independent of the system's masses. On the other hand, the normalized amplitudes in $\underline{\chi}$ always involve the system's masses through the normalization condition (2). We will now derive expressions for numerically computing components of $\underline{A}$ for particles near the impurity and will then consider the zero-frequency normalized defect amplitude $\chi(0x|\lambda = 0)$ itself.

It is useful to return to the general zero-frequency condition (13) and reexpress it in terms of $\underline{A}$ and $\underline{G}_0(0) = \underline{\Phi}_0^{-1}$ as

$$(\underline{I} + \underline{G}_0(0)\Delta\underline{\Phi}_c)\underline{A} = 0 . \tag{34}$$

The localization of $\Delta\underline{\Phi}_c$ allows one to write the same equation for just impurity subspace quantities

$$[\underline{1} + \underline{g}_0(0)\Delta\underline{\phi}_c]\underline{a} = 0 . \tag{35}$$

The matrices $\underline{g}_0(0)$ and $\Delta\underline{\phi}_c$ in our T_{1u} symmetry basis are given by the $z = 0$ limit of Eqs. (23) and (24), provided δ in the latter equation is replaced by the critical value $\delta_c = -(2G_2 - G_1)^{-1}$ implied by the zero-frequency condition $|\underline{1} + \underline{g}_0(0)\Delta\underline{\phi}_c| = 0$. In addition, the impurity-subspace vector $\underline{a}$ is given in this basis by $\tilde{\underline{a}} = [\sqrt{2}A(1x), 1]$. Equation (35) then yields

$$A(1x) = G_1/2G_2 , \tag{36}$$

and through the use of Eq. (34) it is a straightforward matter to derive analogous expressions for the relative amplitudes outside the impurity subspace. The result for sites $n = 1, 2, \ldots$ along the positive x axis is

$$A(nx) = [2G_0(nx, 0x) - G_0(nx, 1x) - G_0(nx, -1x)]/(2G_2) , \tag{37}$$

which reduces to the previous equation for $n = 1$. Symmetry restricts the motion of these particles to the x direction and requires that $A(-nx)$ be equal to $A(nx)$. The defect's four nearest neighbors along the y and z axes also move in just the x direction, as shown in Fig. 2(a), and they have equal amplitudes $A(1'x)$, given by

$$A(1'x) = [G_0(1'x, 0x) - G_0(1'x, 1x)]/G_2 . \tag{38}$$

Equations (37) and (38) are the basis of the numerical calculations of Sec. III B for the zero-frequency relative amplitudes near the impurity.

Turning to the question of the normalized defect amplitude at zero frequency, we note that the $\lambda = 0$ normalization condition (16) for a general harmonic perturbed lattice can be written

$$\chi^{-2}(0x|\lambda = 0) = m_I + S , \tag{39}$$

where S is again the sum defined by Eq. (18). When expressed in terms of the mass matrix $\underline{M}_0$ of the host lattice, S is given by

$$S=\tilde{\underline{A}}\underline{M}_0\underline{A}-m_0, \tag{40}$$

and it will now be shown that for the present model S is equal to F. Using Eq. (34) and the fact that $\underline{G}_0$ and $\Delta\underline{\Phi}_c$ are symmetric matrices, one can rewrite Eq. (40) as

$$S=\underline{\tilde{A}}\Delta\underline{\Phi}_c\underline{G}_0\underline{M}_0\underline{G}_0\Delta\underline{\Phi}_c\underline{A}-m_0\,. \tag{41}$$

Differentiation of the first equation in the definition (3) of $\underline{G}_0(\lambda)$ leads to the identity $D_\lambda\underline{G}_0=\underline{G}_0\underline{M}_0\underline{G}_0$. In writing this, we are anticipating the fact that when the first term of Eq. (41) is worked out, the resulting combinations of elements of $D_\lambda\underline{G}_0$ are well behaved at $\lambda=0$. Furthermore, the vector $\Delta\underline{\Phi}_c\underline{A}$ has nonzero components only in the impurity subspace, and so Eq. (41) becomes

$$S=\tilde{\underline{a}}\Delta\underline{\phi}_c D_\lambda\underline{g}_0\Delta\underline{\phi}_c\underline{a}-m_0\,. \tag{42}$$

This is a general harmonic result.

For the present model, one gets $\tilde{\underline{a}}\Delta\underline{\phi}_c=G_2^{-1}(\sqrt{2}/2,-1)$, and when this result is substituted into Eq. (42) along with $\underline{g}_0$ as given by Eq. (23) for $z=0$, the desired result $S=F$ is obtained. Hence from Eq. (39), the zero-frequency amplitude is determined for this model by the expression

$$\chi^{-2}(0x\,|\,\lambda=0)=m_I+F, \tag{43}$$

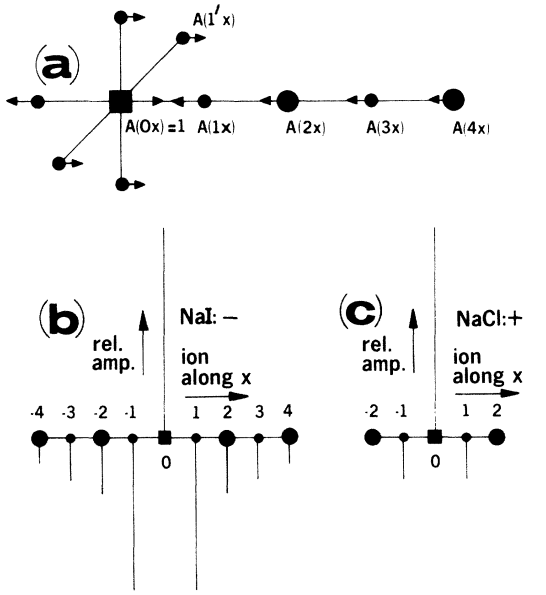

FIG. 2. (a) Schematic representation of the relative amplitudes in the vicinity of the impurity for T_{1u} resonances of zero frequency. Computed values of these amplitudes for the impurity model of Sec. III are given in Table II for a number of systems. In (b) and (c) the calculated relative amplitudes for ions along the x axis are plotted to scale for negative and positive defects in NaI and NaCl, respectively.

and when F is eliminated between this equation and Eq. (30) for the impurity-isotope shift $L(\lambda/\lambda')_I$ in this model, the general harmonic relation (22) of Sec. II B is recovered.

Finally, let us return to the low-frequency resonance condition (28) for the model. We have just seen that F is equal to S, and because S can be written as $S=\tilde{\underline{A}}\underline{M}\underline{A}-m_I$, Eq. (28) is simply $\lambda=\frac{1}{2}(\delta-\delta_c)(G_1/G_2-2)^2/\tilde{\underline{A}}\underline{M}\underline{A}$. Moreover, owing to the localization of $\Delta\underline{\Phi}-\Delta\underline{\Phi}_c$, the quantity $\tilde{\underline{A}}(\Delta\underline{\Phi}-\Delta\underline{\Phi}_c)\underline{A}$ is equal to its impurity subspace counterpart, namely,

$$(\delta-\delta_c)\tilde{\underline{a}}\begin{pmatrix}1 & -\sqrt{2}\\ -\sqrt{2} & 2\end{pmatrix}\underline{a}\,,$$

and this together with the result $\tilde{\underline{a}}=(\sqrt{2}G_1/(2G_2),1)$ leads to the relation $\tilde{\underline{A}}(\Delta\underline{\Phi}-\Delta\underline{\Phi}_c)\underline{A}=\frac{1}{2}(\delta-\delta_c)\times(G_1/G_2-2)^2$. Hence Eq. (28) is verified to be the general harmonic low-frequency resonance condition $\lambda=\tilde{\underline{A}}(\Delta\underline{\Phi}-\Delta\underline{\Phi}_c)\underline{A}/\tilde{\underline{A}}\underline{M}\underline{A}$ of Eq. (14), worked out for this model.

B. Numerical calculations and discussion

It is seen from the preceding work that in order to numerically compute the relative amplitudes and isotope shifts for resonances of very low frequencies, one needs the zero-frequency values of various combinations of elements of the real part of the unperturbed harmonic Green's-function matrix $\underline{G}_0(z)$ for $z=\lambda+i\epsilon$, together with the zero-frequency values of the λ derivatives of these quantities. In the unperturbed crystal the phonons are plane waves, and the mode index f can be written $\vec{k}j$, where $\vec{k}=1,\ldots,N$ labels wave vectors and $j=1,\ldots,s$ denotes polarization branches. Replacing ω^2 in the second equation in (3) by $z=\lambda+i\epsilon$ and going to the limit $\epsilon\to 0^+$ gives

$$\mathrm{Im}\underline{G}_0(\lambda)=\pi\sum_{\vec{k}j}\underline{\chi}(\vec{k}j)\underline{\chi}^\dagger(\vec{k}j)\,\delta(\lambda_{\vec{k}j}-\lambda)\,, \tag{44}$$

where $\lambda_{\vec{k}j}$ is the squared frequency of the unperturbed mode $\vec{k}j$, and the transpose operation in Eq. (3) has been replaced by Hermitian conjugation for the general case of complex $\underline{\chi}(\vec{k}j)$'s. Likewise, the real part of $\underline{G}_0$ is given by

$$P\sum_{\vec{k}j}\underline{\chi}(\vec{k}j)\underline{\chi}^\dagger(\vec{k}j)(\lambda_{\vec{k}j}-\lambda)^{-1}\,,$$

and can be obtained from

$$\mathrm{Re}\underline{G}_0(\lambda)=\pi^{-1}P\int_0^{\lambda_{\max}}dx\,\mathrm{Im}\underline{G}_0(x)(x-\lambda)^{-1}\,. \tag{45}$$

If Eq. (44) is averaged over the squared-frequency interval $(\lambda,\lambda+\Delta\lambda)$ one gets the approximation

$$[\mathrm{Im}\underline{G}_0(\lambda)]_{\mathrm{av}} = \pi(\Delta\lambda)^{-1}\sum_{\vec{k}j}{}' \underline{\chi}(\vec{k}j)\underline{\chi}^{\dagger}(\vec{k}j), \tag{46}$$

with the sum including just modes $\vec{k}j$ for which $\lambda_{\vec{k}j}$ is in the interval. The unperturbed $\underline{\chi}$'s may be written

$$\chi(lb\alpha|\vec{k}j) = N^{-1/2} e(b\alpha|\vec{k}j)\, e^{-i\vec{k}\cdot\vec{R}(lb)}, \tag{47}$$

where the site index has been split into a cell label $l = 1, \ldots, N$ and a basis index $b = b_1, \ldots, b_s$. The polarization vectors $\underline{e}(\vec{k}j)$ are eigenvectors of the host crystal dynamical matrix

$$D(b\alpha, b'\alpha'|\vec{k}) = \sum_{l'} \phi_0(lb\alpha, l'b'\alpha')\, e^{i\vec{k}\cdot\vec{R}(lb,l'b')} \tag{48}$$

and satisfy the orthonormality relation

$$\sum_{b\alpha} m_b e^*(b\alpha|\vec{k}j)\, e(b\alpha|\vec{k}j') = \delta_{jj'} . \tag{49}$$

The vector $\vec{R}(lb, l'b')$ connects the equilibrium positions lb and $l'b'$. With the polarization vectors and squared frequencies of the host crystal at hand, Eq. (46) can be used to compute an approximation to the imaginary part of any desired element of the unperturbed Green's-function matrix, after which Eq. (45) can be used to calculate the corresponding real part.

The calculations to be described here were based upon the frequencies and core polarization vectors of the breathing shell model (BSM) of Schröder.[22] The input parameters of this model are sufficiently few in number that they may be obtained from macroscopic data such as elastic constants, high- and low-frequency dielectric constants, etc., and the agreement between calculated and measured dispersion curves is comparable with that for the shell model (SM) of Cowley *et al.*,[23] which is simply fit to the data. The BSM input data used here is given in Table I of Ref. 24. The unperturbed phonons were computed for a regular mesh of 1686 $\vec{k}$ points in the irreducible $\frac{1}{48}$ element of the Brillouin zone, this being equivalent through symmetry operations to using a mesh of 64 000 $\vec{k}$ vectors in the entire zone. For computing a particular Green's-function element, the interval $(0, \lambda_{\max})$ was divided into 100 bins, each of width $\Delta\lambda = \frac{1}{100}\lambda_{\max}$, and Eq. (46) was used to obtain the average imaginary part for each bin. These values were then associated with the midpoints of the corresponding bins, and the resulting points were connected with straight line segments. With the imaginary part thus approximated, it was then possible to compute analytically the corresponding real part by means of Eq. (45).

Figures 3–6 are plots of the low-frequency behavior of the real part of the quantity $2G_2(z) - G_1(z)$ as computed by the above procedure for positive defects in NaCl, KI, and KBr and for a negative defect in NaI. We recall that the zero-frequency values of this quantity and its derivative with respect to λ play a central role in the nearest-neighbor force constant perturbation model. Moreover, in order for the low-frequency "linear-regime" resonance condition (28) to be valid, the squared resonance frequency must occur in a region where the real part of $2G_2(z) - G_1(z)$ is linear in λ. That this condition is nicely fulfilled for the experimental NaCl:Cu^+, KI:Ag^+, KB:Li^+, and NaI:Cl^- res-

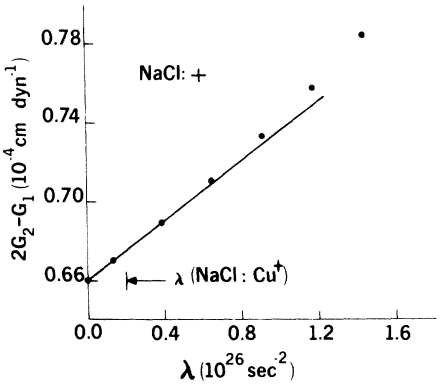

FIG. 3. Unperturbed Green's functions at low frequencies for a positive impurity in NaCl, computed from BSM phonons. The real part of the combination $2G_2(z) - G_1(z)$ of Green's function elements occuring in the defect model of Sec. III is plotted vs $\lambda = \omega^2$. This function's slope at zero frequency is needed for calculating isotope shifts and was obtained from the slope of the straight-line segment shown. The experimental value of λ for NaCl: Cu^+ is indicated.

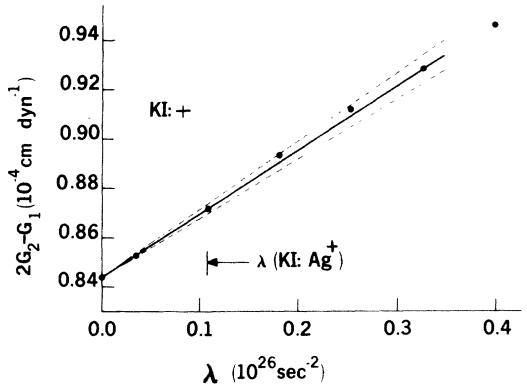

FIG. 4. Same as Fig. 3, but for KI with a positive impurity. The experimental value of λ for KI:Ag^+ is shown. The dotted lines were used in the error estimate for the calculated KI:Ag^+ impurity isotope shift, as discussed in Appendix C.

onances is seen in the figures. In this regard, note that although the plotted points have not been smoothed, they show little scatter. Finally, throughout this paper the imaginary parts of the Green's-function elements have been neglected, and for the above four resonances, the imaginary parts turned out to be down from the corresponding real parts by at least two orders of magnitude. The foregoing considerations insure that the theory of the previous sections may be applied to these resonances.

The zero-frequency derivatives $D_\lambda(2G_2 - G_1)$ were obtained from the slopes of the straight line segments shown in Figs. 3–6. In view of the small scatter and linear behavior exhibited by the computed points at low frequencies, the low frequency points were accorded greater weight in the selection of the line segments. The dotted lines on the KI plot were used for estimating errors in $D_\lambda(2G_2 - G_1)$, as is detailed in Appendix C.

Using the calculated values of $D_\lambda(2G_2 - G_1)$ and G_2 (Ref. 25) to compute the quantity F of Eq. (29), we obtain the values given in the fifth column of Table I. Recall that F is a function of just the force constants and masses of the unperturbed host crystal and that in order for the impurity and host to be effectively decoupled F must be much smaller than the impurity mass. The computed F's are seen to be smaller than the defect mass only for the NaCl:Cu^+ and KI:Ag^+ systems.

Resonance-frequency ratios $[L(\lambda/\lambda')_I]^{1/2}$ were computed for all four systems from Eq. (30) and the results are listed in the fourth column of Table I. It will be recalled that the experimental values are given in the second column, while the third column lists values appropriate to Einstein oscillator, or completely decoupled behavior. The frequency ratios for NaCl:Cu^+ and KI:Ag^+ are seen to be in agreement within the experimental and theoretical uncertainties. On the other hand, the agreement between theory and experiment is very bad for KBr:Li^+ and NaI:Cl^-, the errors in the corresponding fractional frequency *shifts* $\Delta\omega/\omega = \omega_l/\omega_h - 1$ being 85 and 72%, respectively.

Of course, as discussed in Sec. II B, the calculation for KBr:Li^+ was bound to fail since the observed-frequency ratio for this system is greater than that appropriate to Einstein oscillator behavior. Benedek[26] studied anharmonic effects for the KBr:Li^+ system on the basis of a specific model, which although simplified, served to indicate that anharmonicity can play an important role in this system. We have seen that anharmonicity must be included in the theoretical description of KBr:Li^+.

Our calculated frequency ratios for NaCl:Cu^+ and KBr:Li^+ are close to Klein's[3] previously calculated values of 1.013 and 1.019 for these systems, while our ratio for KI:Ag^+ is similar to the value of 1.0065 computed for this system by Benedek and reported in Ref. 8. These authors employed the nearest-neighbor force-constant perturbation model of the defect used here, while their host-crystal phonons were gotten from the shell model of Cowley *et al.*[23] in the case of Klein's work and from the deformation dipole model[27] in the case of Benedek's calculations. Although neither Klein nor Benedek gave estimates of the accuracy of their numerical results, the use of histograms in the calculations of the Green's functions introduces numerical uncertainties which should be estimated if a meaningful comparison between theory and experiment is to be made. Accordingly, simple and somewhat subjective estimates of the uncertainties in our calculated ratios were undertaken, and they are included in Table I. The details of the estimating procedure are found in Appendix C, and a reading of that appendix reveals that the error estimates listed are liberal.

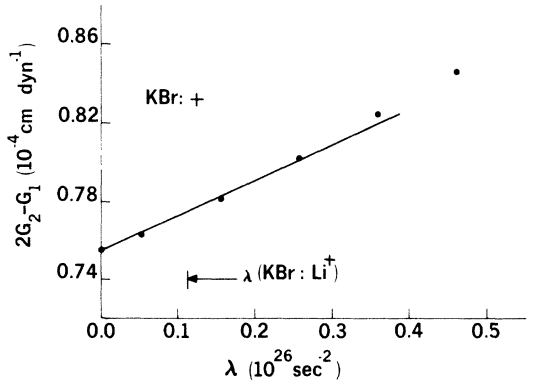

FIG. 5. Same as Fig. 3, but for KBr with a positive impurity. The experimental value of λ for KBr:Li^+ is shown.

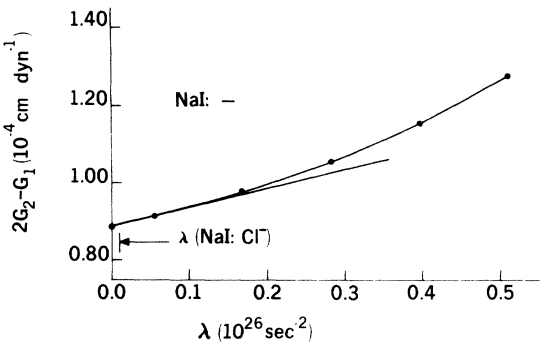

FIG. 6. Same as Fig. 3, but for a negative impurity in NaI. The experimental value of λ for NaI:Cl^- is shown.

TABLE II. Force-constant weakenings and relative amplitudes for impurity-induced T_{1u} resonances of zero frequency in various alkali halides. These quantities are independent of the system's masses and were computed for the defect model of Sec. III, using host-lattice phonons of the breathing shell model[a]. The fractional force constant changes δ_c/k_1 listed here were obtained by dividing δ_c by the value of the unperturbed nearest-neighbor overlap (shell-shell) longitudinal force constant $Ae^2(2v)^{-1}$ of the breathing shell model. The defect displacement is unity.

System	δ_c (10^4dyn cm^{-1})	δ_c/k_1	$A(1x)$	$A(1'x)$	$A(2x)$	$A(3x)$	$A(4x)$
NaCl: +	−1.51	−0.560	−0.204	0.0448	−0.009 54	−0.0144	−0.001 56
NaI: −	−1.13	−0.612	−0.732	0.115	−0.266	−0.199	−0.0716
KCl:+	−1.46	−0.597	−0.369	0.0691	−0.126	−0.0939	−0.0377
KBr: +	−1.33	−0.611	−0.310	0.0543	−0.108	−0.0778	−0.0336
KI: +	−1.19	−0.630	−0.262	0.0464	−0.103	−0.0740	−0.0356

[a]U. Schröder (Ref. 22).

Insight into the isotope shift results may be obtained by calculating the associated amplitude patterns—as we have seen, the tendency towards or away from Einstein-oscillator isotope shifts will be reflected in a greater or lesser tendency for the defect to move alone. For the particles shown in Fig. 2(a), the amplitudes relative to that of the defect were calculated for a zero-frequency resonance within the present model, using Eqs. (37) and (38), for positive and negative defects in several host crystals. It will be remembered that the relative amplitudes are independent of the impurity mass. The results are tabulated in Table II, as are the corresponding values of the force constant changes δ_c leading to zero-frequency resonances in these systems. The calculated amplitude patterns for NaI:− and NaCl:+ are pictorially represented in Figs. 2(b) and 2(c).

It will be noted that there is appreciable motion of the defect's neighbors for all of the systems listed in Table II. The host lattice participates least for the NaCl:+ system, where the defect's nearest neighbors move with 20% of the defect's amplitude, whereas the greatest participation of the host lattice occurs for NaI:−. There the impurity's nearest-neighbor amplitudes are ~70% of that of the defect.

The fact that the ions near the defect are seen to move appreciably in T_{1u} zero-frequency resonances suggests that within this model there could be large lattice distortions in off-center substitutional impurity systems such as KCl:Li^+. Of course our use of the harmonic approximation limits us to small displacements, so that the calculated amplitude patterns do not reflect the state of affairs after such a system achieves its final off-center configuration. Rather, our amplitude patterns describe the motion of a system at the limit of stability for an on-center defect just as it begins to go off center, and thus they describe the distortion associated with the beginning of such a transition. In this regard it is of interest to determine the asymptotic behavior of the relative amplitudes at large distances from the impurity. This is done analytically by means of a simple Debye approximation in Appendix D for ions along the [(100)] directions, and it is seen there that the amplitudes fall off as the inverse cube of the distance from the defect.

In spite of the fact that none of the calculated amplitude patterns reveal isolated defect motion, we have already seen that the associated computed frequency ratios for isotopic defect substitutions in NaCl:Cu^+ and KI:Ag^+ correspond fairly closely to Einstein-oscillator values. To see how this can come about, recall that the connection between the squared-frequency ratios and the relative amplitudes is given by Eq. (17) of Sec. II B, namely,

$$L\left(\frac{\lambda}{\lambda'}\right)_I = \left(m_I' + \sum_{n\neq 0} m(n)A^2(nx)\right) \Big/ \left(m_I + \sum_{n\neq 0} m(n)A^2(nx)\right) .$$

Because the $A(nx)$'s for $n\neq 0$ are less than unity and are squared in this equation, deviations from Einstein-oscillator frequency ratios can be rather insensitive to deviations from Einstein-oscillator amplitude patterns. For instance, in NaCl:+, $A(1,x)$ is approximately -0.2, so that each of the defect's two nearest neighbors along the x axis contributes but 4% of its mass to the effective mass of the mode.

Notice that by truncating the sums in the preced-

ing equation, one can use the calculated relative amplitudes for a subset of particles around the defect to obtain an upper bound on the calculated frequency ratio. As an example, for NaI:Cl^-, the calculated relative amplitudes of just the impurity's two nearest neighbors along the x axis give

$$\left(\frac{\omega_l}{\omega_h}\right)_I < \left(\frac{37+2(23)(-0.732)^2}{35+2(23)(-0.732)^2}\right)^{1/2} = 1.017 .$$

This is somewhat higher than the "exact" calculated value of 1.008 but is already below the experimental value 1.029 ± 0.008, so that knowledge of just the relative amplitudes for the defect's nearest neighbors along the x axis is sufficient to reveal the failure of the present model for this system. The convenience of such an approximation is that only zero-frequency Green's-function elements, but not the derivatives of their real parts, are required to calculate the $A(nx)$'s. As is illustrated in Appendix C for G_1 and G_2, the required zero-frequency Green's function elements can be computed by direct summation. Hence the principal-value sums (45), which must be carried out to compute the derivatives needed for calculating the "exact" ratios of Eq. (30), are avoided.

IV. FURTHER DISCUSSION AND IMPLICATIONS FOR FUTURE WORK

We have seen that the observed isotopic frequency ratio for KBr:$^{6-7}Li^+$ cannot be explained within the framework of any harmonic model. Of the three remaining frequency ratios calculated, those for NaCl:$^{63-65}Cu^+$ and KI:$^{107-109}Ag^+$ are in agreement with the experimental values when account is taken of the computational and experimental uncertainties. Moreover, this agreement is obtained from a model that leaves the defect and lattice coupled at low frequencies, as is revealed by the calculated relative amplitudes of Table II. However, the experimental uncertainties for these two ratios are too large to allow one to make a strong case for the correctness of the nearest-neighbor force-constant perturbation model used here, and by the same token, one is not justified in concluding from the experimental data that these two defect systems exhibit Einstein-oscillator behavior.

The situation for NaI:$^{35-37}Cl^-$ is, however, clear cut—the calculated ratio falls well below the range of experimental values. The assigned experimental ratio of 1.029 is very close to the Einstein-oscillator value of 1.0282, and the large discrepancy between the computed and observed shifts is reflected in the great deviation of the calculated amplitude pattern from that for uncoupled behavior. These results, together with the fact that NaI:Cl^- exhibits the lowest frequency impurity resonance known, suggest that this system should receive major attention in future theoretical work. Directions that future work might take will now be briefly discussed.

A. Improved defect models

Perhaps the most obvious direction would be towards the inclusion of a more realistic set of force constant perturbations. The single-force-constant-change model used here has the virtue of providing a simple yet nontrivial context in which to illustrate the general results of Sec. II and is clearly the model to try first in numerical work. But real impurities can introduce additional force constant changes. For instance, an isoelectronic defect that changes the overlap interaction at the impurity site will perturb the transverse as well as longitudinal nearest-neighbor force constants. The effect of the transverse force-constant changes could be small, however, if the ratio of the transverse to the longitudinal force constants is of the same order, namely, one-tenth,[28] in the perturbed as in the unperturbed crystal.

Another class of realistic force-constant perturbations consists of the long-range changes associated with a defect of altered electronic polarizability. As shown in Refs. 24 and 29 such force-constant changes can be consistently described within a shell model extension of the Green's-function method, and their inclusion could be important for systems such as NaI:Cl^-, where both the Cl^- and I^- ions are polarizable.

A third and possibly the most important class of realistic force-constant perturbations that should be considered consists of changes induced by static distortions about impurities. The substantially weakened force constants necessary to account for the low frequencies of the resonance systems considered in this paper imply that the overlap interactions at the defect sites are considerably less than in the host lattices. Weakened overlap interactions at the defect site will lead to inward relaxations of ions in the defect's vicinity, and theoretical work of the author[21] has shown that these relaxations and the associated force-constant changes between ions of the host crystal can extend quite far from the impurity. The effects of relaxation-induced force-constant changes are known[30] to play an important role in the in-band modes of U centers, but their effects on low-frequency resonances have not yet been studied.

Infrared studies of KI:Ag^+[31,32] and Raman experiments on KI:Ag^+[32] and NaCl:Cu^+[33] in the pres-

ence of an applied electric field have revealed the existence of low-frequency even-parity resonances in these systems, and it turns out that the frequencies of these resonances are not compatible with those of the observed low-frequency T_{1u} resonances within the simple nearest-neighbor longitudinal force-constant change model. This was pointed out in Ref. 31 for KI:Ag^+ on the basis of Benedek and Nardelli's[34] deformation dipole model Green's functions for the appropriate even-parity modes and is also true when breathing shell model Green's functions are used. Additional force-constant changes such as those just discussed could, in principle, account for all of the observed resonances, and they should be studied in future work.

B. Anharmonicity

A major assumption of this paper is the use of the harmonic approximation. Real defects are, of course, anharmonically as well as harmonically coupled to their host lattices, and this results in mode coupling, temperature- and pressure-dependent frequency shifts, lifetime effects, and anharmonic contributions to the $T=0$ frequencies.

Measurements of the effects of temperature, pressure, and electric fields on the NaCl:Cu^+, KI:Ag^+, KBr:Li^+, and NaI:Cl^- resonances have revealed anharmonic properties of these systems. A heuristic phenomenological model has been used by Clayman *et al.*[13] to interpret their second-order Stark effect measurements for the KBr:Li^+ resonance, and in order to explain their results they found it necessary to postulate an effective defect potential well containing a central barrier. This is consistent with our demonstration that no harmonic lattice dynamical calculation can account for the observed isotope shift for this system.

Several properties of the KI:Ag^+ system have been carefully studied by Kirby.[31,32] His observations of even-parity resonances in addition to the 17.4-cm^{-1} T_{1u} resonance, of combination bands involving these resonances, and of electric-field-induced mixing of the odd- and even-parity resonances were shown by him to be semiquantitatively consistent with a simple phenomenological treatment of the resonances as anharmonically coupled harmonic oscillators. This picture was also able to account in a semiquantitative way for the observed[9] uniaxial stress-dependence of the 17.4-cm^{-1} T_{1u} resonance, but was unable to explain the observed[11] temperature dependence of this resonance. Another difficulty was that the model assumed a simple anharmonic coupling term which was treated via perturbation theory, but which turned out to shift the T_{1u} resonance frequency by ~60%. Kirby's results indicate that anharmonicity probably plays an important role in KI:Ag^+, but knowledge of the detailed nature of its role and the determination of its importance in the isotope shift for this system must await realistic lattice dynamical calculations of the sort considered in this paper within the harmonic approximation.

The preceding statement also applies to NaCl:Cu^+, where Raman studies[33] have shown the existence of a low-lying even-parity resonance that appears to be anharmonically coupled with an even parity overtone of the 23.6-cm^{-1} T_{1u} resonance. More direct information on the anharmonic properties of the T_{1u} resonance itself is obtained from its observed[35,11] temperature dependence. Timmesfeld[36] was able to successfully account for the temperature dependence by means of an anharmonic self-energy calculation in which the anharmonicity appears to play little role near $T=0$. This suggests that the 23.5-cm^{-1} resonance in NaCl:Cu^+ may be treated harmonically at very low temperatures.

Turning finally to the 5.4-cm^{-1} resonance in NaI:Cl^-, we note that second-order Stark-effect measurements by Clayman *et al.*[13] were successfully interpreted by these authors in terms of a phenomenological model that considers the defect to be moving in a static three-dimensional harmonic potential well which is weakly perturbed by quartic anharmonic terms appropriate to a site of O_h symmetry. Fitting the parameters of this simple model to some of their data, these authors were able to explain consistently all of their measurements. The anharmonic contribution to the resonance frequency in their model turned out to be just 7% or < 0.4 cm^{-1}. Moreover, their calculated NaI:$^{35-37}Cl^-$ frequency ratio was $\omega_l/\omega_h = 1.030$, which is nearly equal to the Einstein-oscillator value of 1.028 that is necessarily predicted by their model when anharmonicity is neglected. Anharmonicity thus turned out to be small in the model of Clayman *et al.*, and although their model must be regarded as heuristic, its success in giving a coherent picture of their experimental results suggests that a proper lattice dynamical investigation of the 5.4-cm^{-1} resonance in NaI:Cl^- may be validly carried out within the harmonic approximation. This is yet another indication that major emphasis should be placed on the NaI:Cl^- resonance in future extensions of the work of this paper.

V. SUMMARY

In this paper the properties of harmonic impurity resonances and associated isotope effects

have been investigated in the asymptotic limit of low frequencies.

In Sec. II it was shown how mode effective masses and force constants can be defined in terms of particle amplitudes relative to that of the impurity, and a general relation was derived that connects these amplitudes to resonance frequency ratios for isotopic substitutions of the defect. This relation is independent of the model of the defect and shows that these frequency ratios must always be bounded above by ratios appropriate to the defect behaving as an Einstein oscillator. The necessary as well as sufficient condition for Einstein-oscillator ratios is that the impurity moves alone—thus the possibility of a complicated force constant model with fortuitous cancellations leading to Einstein oscillator ratios but with nonzero host lattice amplitudes is impossible within the harmonic approximation. From the fact that the observed ratio for KBr:Li^+ is greater than the Einstein oscillator value, we could thus rule out the possibility of any explanation of the defect isotope shift of this system within the harmonic approximation.

In Sec. III, the general results of Sec. II were illustrated for an explicit model of the defect. This necessitated the use of Green's-function approach to perturbed lattice dynamics, and the formulas so obtained were applied in numerical calculations for isoelectronic defects in several alkali halides, using realistic host-crystal phonons. The single force constant perturbation model used in these calculations resulted in computed defect-isotope shifts smaller than those for Einstein-oscillator behavior, and calculations of the relative amplitudes in the vicinity of the defects showed graphically why this was so: in this model there is enough motion of the defect's surroundings for the mode's effective mass to involve significant contributions from masses other than that of the impurity. When account was taken of computational and experimental uncertainties, the calculated and measured isotope frequency ratios were in agreement for NaCl:Cu^+ and KI:Ag^+ within this simple model. However, it was also seen that the experimental uncertainties for these ratios are large enough that this agreement may be fortuitous, and as discussed in Sec. IV, more recent experimental studies of properties other than isotope shifts suggest that these two systems should be described by more complicated force constant perturbations than those used here.

The NaI:Cl^- system was perhaps the most interesting system considered. The model calculations revealed a very extensive coupling between defect and host at low frequencies, and the computed isotopic-frequency ratio was correspondingly well below the range of measured values. Experimental evidence that anharmonicity may play but a small role in the isotope shift for this system was discussed in Sec. IV, and we have suggested that this system receive future theoretical emphasis, with an eye towards more realistically treating the harmonic defect perturbations, especially those associated with defect-induced lattice distortions and defect polarizability.

Anharmonicity has been neglected in our work and has been experimentally shown to be important for some properties of low-lying defect resonance systems, as discussed in Sec. IV. However, its importance for isotope effects remains to be demonstrated, except for KBr:Li^+.

Whether or not anharmonicity is important for particular systems, it is imperative that the general asymptotic properties of low-frequency harmonic resonsnces be well understood before one undertakes the study of anharmonic effects. This paper has resolved the apparently conflicting conclusions of earlier studies carried out within the harmonic approximation and referred to in Sec. I. The results obtained here give insight into the behavior of low-frequency impurity resonances and should provide a useful basis for future work.

ACKNOWLEDGMENTS

It is a pleasure to acknowledge stimulating discussions on various phases of this work with Professor J. A. Krumhansl, Professor A. J. Sievers, and Dr. D. Strauch, and to thank Professor J. A. Krumhansl and Professor H. Bilz for their hospitality during extended stays of the author at Cornell University and the Technische Universität, Müchen, where some portions of this work were begun.

APPENDIX A: LOW-FREQUENCY BEHAVIOR OF THE UNPERTURBED GREEN'S FUNCTIONS

According to Eq. (44), the imaginary part of the unperturbed Green's-function matrix for squared frequency λ is given by

$$\mathrm{Im}\underline{G}_0(\lambda) = \pi \sum_{\vec{k}j} \underline{\chi}(\vec{k}j)\underline{\chi}^{\dagger}(\vec{k}j)\delta(\lambda_{\vec{k}j} - \lambda) .$$

The elements of this matrix are seen to be weighted densities of squared frequencies, with the weighting factors consisting of products of vibrational amplitudes. Since the density of squared frequencies vanishes in the $\lambda \to 0$ limit, so do the elements of $\mathrm{Im}\underline{G}_0(\lambda)$.

On the other hand, the real part of the unperturbed Green's-function matrix for squared frequency λ is given by Eq. (45) as

$$\mathrm{Re}\underline{G}_0(\lambda)=\pi^{-1}P\int_0^{\lambda_{\max}}dx\,\mathrm{Im}\underline{G}_0(x)(x-\lambda)^{-1},$$

and for arbitrary $\mathrm{Im}\underline{G}_0(x)$, this generally will not vanish as λ approaches zero.

We now use a simple Debye model to investigate, in the $\lambda\to 0$ limit, the frequency dependence of the real and imaginary parts of the combinations $G_1(z)$ and $G_2(z)$ of Green's-function elements involved in the model of Section III. These combinations are $G_1(z)=2G_0(0x,1x;z)-G_0(1x,1x;z)-G_0(1x,-1x;z)$ and $G_2=G_0(0x,0x;z)-G_0(0x,1x;z)$, where z is equal to $\lambda+i\epsilon$. Through the use of Eqs. (44) and (47), we have

$$\mathrm{Im}G_1(\lambda)=\pi N^{-1}\sum_{\vec{k}j}\{2e(0x|\vec{k}j)e(1x|\vec{k}j)\cos\vec{k}\cdot\vec{R}(0,1)-e^2(1x|\vec{k}j)[1+\cos\vec{k}\cdot\vec{R}(1,-1)]\}\delta(\lambda_{\vec{k}j}-\lambda)$$

and

$$\mathrm{Im}G_2(\lambda)=\pi N^{-1}\sum_{\vec{k}j}[e^2(0x|\vec{k}j)-e(0x|\vec{k}j)e(1x|\vec{k}j)\cos\vec{k}\cdot\vec{R}(0,1)]\delta(\lambda_{\vec{k}j}-\lambda).$$

In arriving at these expressions use has been made of the fact that the polarization vectors may be taken to be purely real for crystals having inversion symmetry. Notice that since the $k=0$ acoustic modes correspond to uniform translations and hence involve site-independent polarization vectors, the contributions to the above quantities from these modes are zero.

As λ approaches zero, only the low-frequency acoustic modes contribute to $\mathrm{Im}G_1(\lambda)$ and $\mathrm{Im}G_2(\lambda)$. For these modes we will: a) neglect the $\vec{k}$-dependence of the polarization vectors so that they may be replaced by their $k=0$ values, which are site-independent as just mentioned; and b) assume that the three acoustic branches are degenerate and Debye-like so that $\lambda_{\vec{k}j}=v^2k^2$. When these approximations are incorporated into the preceding equations for $\mathrm{Im}G_1$ and $\mathrm{Im}G_2$ and these equations are averaged over an interval $(\lambda,\lambda+\Delta\lambda)$ as in Eq. (46), one obtains

$$[\mathrm{Im}G_1(\lambda)]_{\mathrm{av}}\propto(\Delta\lambda)^{-1}\sum_{\vec{k}}{}'[2\cos\vec{k}\cdot\vec{R}(0,1)-1-\cos\vec{k}\cdot\vec{R}(1,-1)]$$

and

$$[\mathrm{Im}G_2(\lambda)]_{\mathrm{av}}\propto(\Delta\lambda)^{-1}\sum_{\vec{k}}{}'[1-\cos\vec{k}\cdot\vec{R}(0,1)],$$

where the sums go over just those $\vec{k}$'s for which $\lambda_{\vec{k}j}=v^2k^2$ is in the interval. The sums thus extend over a spherical shell $(k,k+\Delta k)$ in $\vec{k}$ space, and integration over the shell leads to

$$[\mathrm{Im}G_1(\lambda)]_{\mathrm{av}}\propto(\Delta k/\Delta\lambda)[2R^{-1}(0,1)k\sin kR(0,1)-k^2-kR^{-1}(1,-1)\sin kR(1,-1)]$$

and

$$[\mathrm{Im}G_2(\lambda)]_{\mathrm{av}}\propto(\Delta k/\Delta\lambda)\times[k^2-kR^{-1}(0,1)\sin kR(0,1)].$$

Now by expanding about $k=0$ and using the relations $\Delta k/\Delta\lambda=(2kv^2)^{-1}$ and $R(1,-1)=-2R(0,1)$, one finds that the leading term in each of these expressions is of order k^3. Hence both $\mathrm{Im}G_1(\lambda)$ and $\mathrm{Im}G_2(\lambda)$ are proportional to $\lambda^{3/2}$ in the $\lambda\to 0$ limit. This is to be contrasted with the low-frequency behavior of the *individual* Green's-function elements, which by a similar calculation are found to go as $\lambda^{1/2}$ in this model.

Turning now to the low-frequency behavior of $\mathrm{Re}G_1(\lambda)$ and $\mathrm{Re}G_2(\lambda)$, we have

$$\mathrm{Re}G_1(\lambda)=\pi^{-1}P\int_0^{\lambda_{\max}}\mathrm{Im}G_1(x)(x-\lambda)^{-1}dx$$

and a similar equation for $\mathrm{Re}G_2(\lambda)$. If the region of integration is split into two intervals $(0,a)$ and $(a,\lambda_{\max})$, where $(0<\lambda<a)$, we have

$$\mathrm{Re}G_1(\lambda)=\pi^{-1}P\int_0^a dx\,\mathrm{Im}G_1(x)(x-\lambda)^{-1}+\pi^{-1}\int_a^{\lambda_{\max}}dx\,\mathrm{Im}G_1(x)(x-\lambda)^{-1},$$

with only the first term involving a principal-value integral. We have seen that as λ approaches zero, $\mathrm{Im}G_1(\lambda)$ goes to zero as $\lambda^{3/2}$. Hence in this limit a can be chosen sufficiently small that we can write $\mathrm{Im}G_1(x)=Ax^{3/2}$ in the interval $(0,a)$, where A is a constant. This gives

$$\mathrm{Re}G_1(\lambda)=\pi^{-1}AP\int_0^a dx\,x^{3/2}(x-\lambda)^{-1}+\pi^{-1}\int_a^{\lambda_{\max}}dx\,\mathrm{Im}G_1(x)(x-\lambda)^{-1}.$$

The first integral is straightforward to perform, and to first order in λ one obtains

$$\mathrm{Re}G_1(\lambda) = (3\pi)^{-1} 2Aa^{3/2}(1+3a^{-1}\lambda) + \pi^{-1}\int_a^{\lambda_{\max}} dx\, \mathrm{Im}G_1(x)x^{-1} + \lambda\pi^{-1}\int_a^{\lambda_{\max}} dx\, \mathrm{Im}G_1(x)x^{-2}.$$

Since a is arbitrary within the restrictions previously stated, the above equation is sufficient to establish that $\mathrm{Re}G_1(\lambda)$ is linear in λ and, furthermore, approaches a nonzero value as λ approaches zero. The argument and conclusions for $\mathrm{Re}G_2(\lambda)$ are exactly the same.

APPENDIX B: MODEL OF SIEVERS AND TAKENO

In the model of Sievers and Takeno, [17] referred to subsequently as (ST), the host crystal is assumed to be a simple cubic monatomic lattice of atoms of mass m interacting by means of equal longitudinal and transverse force constants $k_l = k_t \equiv k$ between nearest neighbors. The defect is assumed to introduce a changed mass m_I and altered force constants $k_{lI} = k_{tI} \equiv k_I$ to each of its six nearest neighbors. For this model the condition for a resonance at squared frequency $\lambda = \omega^2$ is

$$0 = \mathrm{Re}|\underline{1} + \underline{g}_0(z)\underline{c}(z)| = \frac{k_I}{k} + 2\frac{m_I}{m}\left(\frac{k_I}{k} - 1\right)\frac{\lambda}{\lambda_D} + \left[\frac{k_I}{k}\left(\frac{m_I}{m} - 1\right) - 2\frac{m_I}{m}\left(\frac{k_I}{k} - 1\right)\frac{\lambda}{\lambda_D}\right]\lambda g(\lambda), \tag{B1}$$

where $\lambda_D = 12k/m$ is the maximum squared frequency of the unperturbed host crystal and $g(\lambda)$ is the real part of the defect-site Green's function. The condition for a zero-frequency resonance in this model is seen to be $k_I = 0$, as is obvious physically since k_I is the value of the only force constants which couple the defect to the host.

The condition for a low-frequency resonance will now be derived by working out Eq. (B1) to second order in the small quantities λ and k_I. To this order, $g(\lambda)$ is only needed at zero frequency, and ST show that in the Debye approximation $g(0)$ is equal to $-3\lambda_D^{-1}$. Using this result in Eq. (B1), we obtain, to second order,

$$\frac{\lambda}{\lambda_D} = \frac{1}{2}\frac{m}{m_I}\left(\frac{k_I}{k}\right)\left[1 - \frac{1}{2}\left(\frac{k_I}{k}\right)\right]. \tag{B2}$$

The first-order approximation

$$\lambda/\lambda_D = \tfrac{1}{2}(m/m_I)k_I/k$$

is just our general harmonic first-order resonance condition (14), worked out for the ST model.

According to Eq. (B2), the ratio of squared frequencies for an isotopic substitution $m_I \to m_I'$ of the defect is given by the Einstein-oscillator value $(\lambda/\lambda')_I = m_I'/m_I$ for either the first- or second-order resonance conditions. That the first-order condition yields this value is consistent with our general harmonic result (19) and, furthermore, is easy to understand intuitively: in the ST model a zero-frequency resonance is achievable only by letting k_I approach zero, in which case the defect and host become completely decoupled.

ST started from Eq. (B1) and derived an approximate low-frequency resonance condition that differs from our approximation (B2). Their result is

$$\left(\frac{\lambda}{\lambda_D}\right)_{\mathrm{ST}} = \frac{1}{2}\frac{m}{m_I}\left(\frac{k_I}{k}\right)\left[1 + \frac{1}{2}\left(\frac{k_I}{k}\right)\left(1 - 3\frac{m}{m_I}\right)\right]^{-1} \tag{B3}$$

and it is seen to agree with Eq. (B2) only to first order. As pointed out by Kirby *et al.*[8] the above resonance condition leads to ratios $(\lambda/\lambda')_I$ *greater* than the Einstein-oscillator values m_I'/m_I. This is seen to be due to the fact that the ST low-frequency resonance condition (B3) includes some, but not all, terms of second order. Indeed, some terms of *all* orders are included in Eq. (B3), and it is the nonlinear terms which produce the anomalous isotope shifts.

To summarize, when the resonance condition for the ST model is worked out to first order, one obtains Einstein-oscillator defect-isotope shifts, which are, of course, consistent with our general harmonic theory. In addition, we have also shown that when the resonance condition for the ST model is worked out correctly even to second order, Einstein-oscillator defect-isotope shifts again result.

APPENDIX C: THEORETICAL UNCERTAINTY ESTIMATES

As an illustration of the procedure used to estimate the uncertainties in the calculated frequency ratios for impurity-isotope substitutions, consider the case of KI:Ag^+, which is typical. Let the basic calculated quantity $D_\lambda(2G_2 - G_1)/(2G_2^2)$ of F be written $[T(\lambda) - T(0)]/(\lambda 2G_2^2)$, where $T(\lambda)$ represents the straight line segment used for evaluating the slope $D_\lambda(2G_2 - G_1)$ from Fig. 4. Estimates are needed of $T(\lambda)$ and of the zero-frequency quantities G_2 and $T(0) = 2G_2 - G_1$.

Now although the Green's function have been computed by approximating the imaginary parts as histograms and then calculating the corresponding real parts by taking Hilbert transforms as

outlined previously, this procedure can be bypassed for the real parts of $G_1(z)$ and $G_2(z)$ at zero frequency, which can be evaluated by direct summation. Thus from Eqs. (45) and (47) we have, for instance,

$$G_2 = \lim_{\lambda \to 0} N^{-1} P \sum_{\vec{k}j} [e^2(0x|\vec{k}j) - e(0x|\vec{k}j)e(1x|\vec{k}j) \times \cos\vec{k}\cdot\vec{R}(0,1)](\lambda_{\vec{k}j} - \lambda)^{-1}$$

$$= N^{-1} \sum_{\vec{k}j} [e^2(0x|\vec{k}j) - e(0x|\vec{k}j)e(1x|\vec{k}j) \times \cos\vec{k}\cdot\vec{R}(0,1)]\lambda_{\vec{k}j}^{-1},$$

where use has been made of the fact that the polarization vectors may be taken to be purely real for crystals having inversion symmetry. The $k=0$ acoustic modes do not contribute to this sum since for them the term in square brackets vanishes, as was also pointed out in Appendix A. Evaluating the zero frequency quantities G_2 and $T(0)$ by direct summation, then, and comparing the results with those obtained from taking Hilbert transforms of the imaginary parts gives an estimate of the statistical uncertainties in these quantities. In this way we find for KI: + a fractional uncertainty in G_2 of 7.8×10^{-4} and a fractional uncertainty in $2G_2 - G_1$ of 1.3×10^{-4}. In estimating the fractional uncertainty in F, each of the above uncertainties was rounded up to 10^{-3}.

To complete the error estimation, one needs the uncertainty in $T(\lambda)$ which represents the straight-line segment in Fig. 4. Since according to the preceding paragraph the uncertainty in $T(0)$ is at most one part per thousand, it can be seen by referring to Fig. 4 that the main contribution to error in $T(\lambda)$ arises from uncertainty in the choice of slope of the straight line. It is felt that the dotted lines shown on Fig. 4 give a fairly liberal estimate of the range of slopes of $T(\lambda)$, although the choice is admittedly somewhat subjective, especially in view of the fact that the low-frequency points are accorded greater weight, as discussed in Sec. III B. The dotted lines shown yield a fractional uncertainty in $T(\lambda)$ of 6.5×10^{-3} at $\lambda = 0.34 \times 10^{26}$ sec^{-2}.

From these estimates one finds that the fractional error in $D_\lambda(2G_2 - G_1)/(2G_2^2)$ for KI:Ag$^+$ is 8.1×10^{-2}, from which the error in the calculated isotope ratio for KI:Ag$^+$ turns out to be 2.9×10^{-4}. This has been rounded up to 3×10^{-4}, the value given in Table I. A similar procedure was followed in estimating the theoretical errors for the other three ratios of Table I.

APPENDIX D: BEHAVIOR OF $A(nx)$ AT LARGE DISTANCES

The asymptotic form of the relative amplitudes at large distances along the x axis for a zero-frequency x-polarized T_{1u} resonance will now be worked out for the model of Sec. III, within the same Debye approximation used in Appendix A.

According to Eqs. (37), (45), and (47), the relative amplitude $A(nx)$ of the nth particle from the defect along the x axis is proportional to the quantity

$$\sum_{\vec{k}j} \{2e(nx|\vec{k}j)e(0x,\vec{k}j)\cos\vec{k}\cdot\vec{R}(n,0) - e(nx|\vec{k}j)e(1x|\vec{k}j)[\cos\vec{k}\cdot\vec{R}(n,1) + \cos\vec{k}\cdot\vec{R}(n,-1)]\}\lambda_{\vec{k}j}^{-1}.$$

As in Appendices A and C, use has been made of the fact that the polarization vectors may be taken to be purely real for crystals having inversion symmetry. Moreover, by an argument analogous to that given for G_2 in Appendix C, the $k=0$ acoustic modes do not contribute to the sum.

To get the asymptotic R dependence of the above quantity, we ignore the contributions of the optical modes and treat the acoustic modes within the simple Debye approximation of Appendix A. Thus, we neglect the $\vec{k}$ dependence of the polarization vectors so that they may be replaced by their $k=0$ values, which are site independent, and we assume that the three acoustic branches are degenerate and Debye-like so that $\lambda_{\vec{k}j} = v^2k^2$. Then within these approximations $A(nx)$ is seen to be proportional to

$$\sum_{\vec{k}} [2\cos\vec{k}\cdot\vec{R}(n,0) - \cos\vec{k}\cdot\vec{R}(n,1) - \cos\vec{k}\cdot\vec{R}(n,-1)]k^{-2}.$$

Converting the sum to an integral over the Debye sphere and letting the R's be large compared with the nearest-neighbor distance r_0 gives

$$A(nx) \propto 2R^{-1}(n,0) - R^{-1}(n,1) - R^{-1}(n,-1).$$

Now $R(n,1)$ and $R(n,-1)$ are given by $R(n,0) - r_0$ and $R(n,0) + r_0$, respectively, and expansion in powers of $r_0/R(n,0)$ leads to

$$A(nx) \propto \frac{1}{R(n,0)}\left(\frac{r_0}{R(n,0)}\right)^2 + \text{higher-order terms}.$$

Hence, within the model of Sec. III and the above approximations, the relative amplitudes associated with a zero-frequency resonance fall off with distance from the defect as R^{-3}.

*Work supported by the National Science Foundation under Grant No. GH-34248.

[1]R. Brout and W. M. Visscher, Phys. Rev. Lett. 9, 54 (1962).
[2]A. A. Maradudin, in *Solid State Physics*, edited by F. Seitz and D. Turnbull (Academic, New York, 1966), Vols. 18 and 19.
[3]M. V. Klein, in *Physics of Color Centers*, edited by W. Beall Fowler (Academic, New York, 1968), p. 429.
[4]A. A. Maradudin, E. W. Montroll, G. H. Weiss, and I. P. Ipatova, *Theory of Lattice Dynamics in the Harmonic Approximation 2nd ed.* (Academic, New York, 1971).
[5]*Localized Excitations in Solids*, edited by R. F. Wallis (Plenum, New York, 1968).
[6]A. J. Sievers, Phys. Rev. Lett. 13, 310 (1964).
[7]R. Weber, Physics Lett. 12, 311 (1964).
[8]R. D. Kirby, I. G. Nolt, R. W. Alexander, Jr., and A. J. Sievers, Phys. Rev. 168, 1057 (1968).
[9]I. G. Nolt and A. J. Sievers, Phys. Rev. 174, 1004 (1968).
[10]B. P. Clayman, I. G. Nolt, and A. J. Sievers, Solid State Commun. 7, 7 (1969).
[11]R. W. Alexander, Jr., A. E. Hughes, and A. J. Sievers, Phys. Rev. B 1, 1563 (1970).
[12]R. D. Kirby, A. E. Hughes, and A. J. Sievers, Phys. Rev. B 2, 481 (1970).
[13]B. P. Clayman, R. D. Kirby, and A. J. Sievers, Phys. Rev. B 3, 1351 (1971).
[14]H. S. Sack and M. C. Moriarty, Solid State Commun. 3, 93 (1965); G. Lombardo and R. O. Pohl, Phys. Rev. Lett. 15, 291 (1965).
[15]J. A.Krumhansl, in Ref. 5, p. 17.
[16]J. A. Krumhansl and J. A. D. Matthew, Phys. Rev. 166, 856 (1968).
[17]A. J. Sievers and S. Takeno, Phys. Rev. 140, A1030 (1965).
[18]G. Benedek and G. F. Nardelli, Phys. Rev. 155, 1004 (1967).
[19]I. M. Lifschitz, Nuovo Cimento Suppl. 3, 716 (1956).
[20]See, for instance, J. B. Page, Jr., Phys. Rev. 184, 905 (1969).
[21]J. B. Page, Jr., Bull. Am. Phys. Soc. 15, 339 (1970).
[22]U. Schröder, Solid State Commun. 4, 347 (1966).
[23]R. A. Cowley, W. Cochran, B. N. Brockhouse, and A. D. B. Woods, Phys. Rev. 131, 1030 (1963).
[24]J. B. Page, Jr. and D. Strauch, Phys. Status Solidi 24, 469 (1967).
[25]The computed values of the zero-frequency quantities G_1 and G_2 are not listed here explicitly, but they may be easily inferred from the calculated values of $\delta_c = -(2G_2 - G_1)^{-1}$ and $A(1x) = G_1/(2G_2)$ given in the first and third columns of Table II.
[26]G. Benedek, in Ref. 5, p. 101.
[27]J. R. Hardy, Philos. Mag. 7, 315 (1962).
[28]For instance, in NaI $|B/A|$ is equal to 0.0965 in the breathing shell model.
[29]J. B. Page, Jr., and D. Strauch, in Ref. 5, p. 559; D. Strauch and J. B. Page, Jr., *ibid.*, p. 567.
[30]T. Gethins, T. Timusk, and E. J. Woll, Phys. Rev. 157, 744 (1967).
[31]R. D. Kirby, Phys. Rev. Lett. 26, 512 (1971).
[32]R. D. Kirby, Phys. Rev. B 4, 3557 (1971).
[33]B. N. Ganguly, R. D. Kirby, M. V. Klein, and G. P. Montgomery, Jr., Phys. Rev. Lett. 28, 307 (1972).
[34]G. Benedek and G. F. Nardelli, J. Chem. Phys. 48, 5242 (1968).
[35]R. Weber and P. Nette, Phys. Lett. 20, 493 (1966).
[36]K. H. Timmesfeld, Phys. Status Solidi 30, 73 (1968).